Study of ELMy H-mode plasmas and BOUT++ simulation on EAST

Z.X. Liu[1], X. Gao[1], X.Q. Xu[2], T.Y. Xia[1,2], S.C. Liu[1] and J.G. Li[1]

[1]Institute of Plasma Physics, Chinese Academy of Sciences, Hefei 230031, China
[2]Lawrence Livermore National Laboratory, Livermore, CA94550, USA

Corresponding Author: zxliu316@ipp.ac.cn

Abstract:

A series of ELMing H-mode discharges have been achieved on Experimental Advanced Superconducting Tokamak (EAST) combine with Low Hybrid Wave ($P_{LHW} = 1 \sim 2MW$ at 2.45 GHz) and Ion cyclotron resonance frequencies ($P_{ICRF} = 1MW$) in 2012. Experimental threshold power in this campaign appears to be in a lower state compared with the scaling law P_{thr_cal08}. Significant reduction in H-mode threshold power with the lowered X-point has proven in the lower single configuration, and the lowered X-point configuration is much closer to the double null. A significant reduction (about 23%) in the H-mode threshold power is achieved. BOUT++ simulation has been calculated using the EAST experimental data. The simulation result shows ELMs at low toroidal mode number becomes dominant when the plasma current increases. The structure of the ELMs has been studied by a CCD camera, and the result is in agreement with the simulation.

1 Introduction

Since the first experimental demonstration of H-mode [1], the low-to-high confinement transition (L–H) studies have attracted considerable research efforts and the problem of prediction for threshold power of L-H transition in fusion devices has raised considerable interest for a long time and there is no established theory for the prediction. The transition may be affected by many influences[2, 3, 4, 5, 6]. The early results of the threshold power of the L-H transition on EAST have been reported[7]. The toroidal field of the H-mode shots in 2010 is clockwise from the bird's-eye view. This year the toroidal field has been changed into anti-clockwise, so the ∇B drift towards upper side which is opposite to the experiments in 2010. Type III H-mode has been observed in double-null and lower single-null configuration and the threshold power has been studied in this paper.

Type I ELM is successfully explained by ideal peeling-ballooning (P-B) theory in pedestal [8], in which the steep pressure gradients drive ballooning mode and bootstrap current generates peeling mode. The fast-reconnection simulation of ELMs in high-confinement mode tokamak discharges with non-ideal physics effects has been reported by Xu, et al [9]. The linear understanding of P-B mode is well developed by numerical

codes, such as ELITE[10, 11] and GATO [12]. and also some 3D codes have been developed for the nonlinear simulation of ELMs, including NIMROD [13, 14], BOUT [15, 16], JOREK [17], etc. BOUT++ code has successfully simulated the nonlinear crash phase of ELMs [9, 19]. EAST experimental data such as density profile (measured by reflectomter), electron temperature profile (measured by Thomson scattering[20]), and the magnetic geometry (calculated by EFIT) have been used as the input parameters of the BOUT++ simulation code. The Thomson scattering measures the electron temperature from Z=-4.1 cm to 61.1 cm at R=1.91 m, where Z is the vertical distance from the mid-plane. The uncertainty of Z is about 1mm. The reflectometer measured the density at the mid-plane. The pedestal top position is fixed by Thomson scattering and the density at the separatrix is diagnosed by Langmuir probe. This paper shows the simulation calculation, and shows relevant experiment results.

2 Threshold power

EAST, as a full superconducting tokamak, is aimed at long pulse ($60 \sim 1000s$) high performance operation. A water cooled molybdenum wall has replaced the graphite wall in EAST since 2012 as shown in Fig. 1(a). H-mode threshold power is characterized by the total power loss to the plasma boundary, which is defined according to [21] as $P_{loss} = P_{tot} - dW/dt = P_{oh} + P_{aux} - dW/dt$ where P_{oh} is ohmic power, P_{aux} is the absorbed power contributed by LHW on EAST and dW/dt is the time variation of the total plasma energy. The net power loss, $P_{net} = P_{th} - P_{rad}$, may be a more appropriate quantity to characterize the H-mode threshold power. Upon an examination, the P_{rad} for the discharges are mostly about 10% of the P_{aux} and essentially independent of density. So the overall trend of P_{net} is basically differed from that of P_{th} by an offset.

Early studies were focused on assembling data of P_{th} from multiple devices into a database and extracting an empirical scaling law with global plasma parameters out of it[22]. These works yielded the international tokamak scaling as follows:

$$P_{thr\_cal08} = 0.0488 e^{\pm 0.057} n_{e20}^{0.717 \pm 0.035} B_T^{0.803 \pm 0.032} S^{0.941 \pm 0.019}, \quad (1)$$

which indicates that the three primary dependences of P_{th} are plasma density, strength of toroidal magnetic field and plasma surface area. The experimental threshold power (P_{loss}) increases with the plasma density in Fig. 1(b), and all the data are below the scaling law. According to the experimental result of EAST in 2010[7], the experimental threshold power is almost above the scaling law. All the data we selected is based on the double null configuration and the LHW as the heating power. Experiment on EAST in 2012 has only two significant differences from them in 2010. One is the material of the first wall (graphite wall in 2010; molybdenum wall in 2012), and the other is the direction of the toroidal field (counter-I_p in 2010; co-I_p in 2012). Lower P_{th} in Be/W wall than in Carbon wall has been observed in JET reported by C.F. Maggi in the latest ITPA TC group meeting in Hefei, which might be the cause of the lower threshold power on EAST.

The influence of the threshold power by changing the distance between the X-point and the strike-point at outside lower divertor has observed on EAST in 2012. Significant

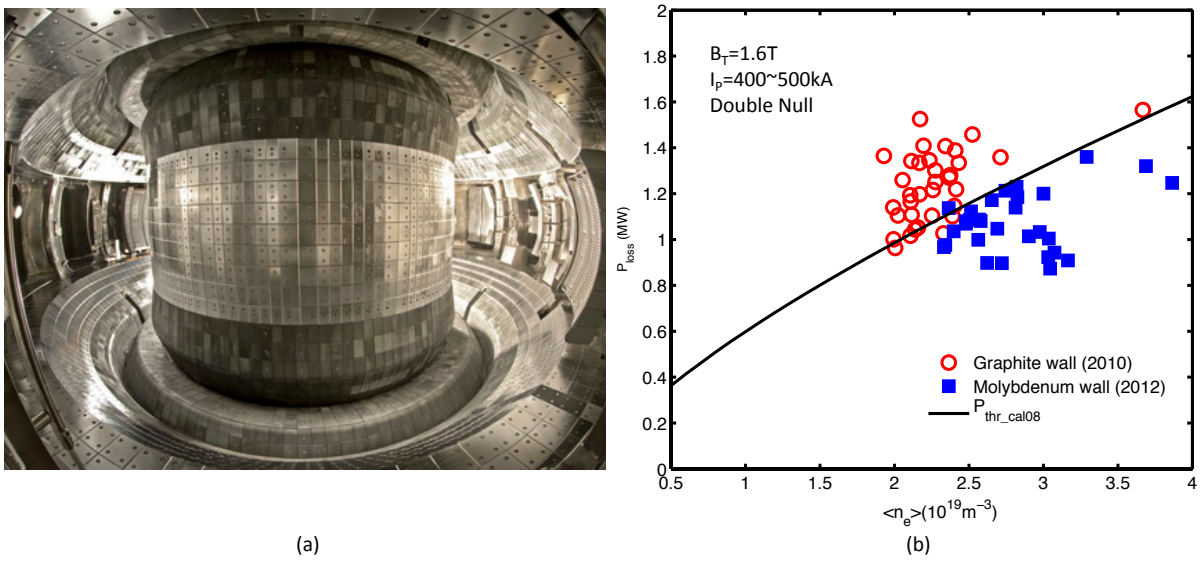

FIG. 1: (a) Picture of the EAST in-vessel with water cooled molybdenum wall. (b)Threshold power as a function of plasma density n_e with toroidal field B_T=1.6T. Red open circle is 2010 data with graphite wall, and blue solid square is 2012 data with Molybdenum wall. The solid black line is the threshold power at 1.6T predicted by the scaling law (P_{thr_cal08}).

reduction in H-mode threshold power with the lowered X-point (shot: 38628) has proven in the lower single configuration. An reduction (about 23%) in H-mode threshold power with the lowered X-point has been investigated by decreasing the X-point by 3.4cm. In EAST, magnetic divertor balance is described by dRsep=the radial separation at the low-field side midplane between the flux surfaces connected to the upper and lower divertor X-points. An upper single-null plasma has been defined by dRsep¿1cm , lower single-null has dRsep¡-1cm , and double-null (DN) has dRsep between -1cm to 1cm. Figure 2 shows the threshold power divided by plasma density as a function of dRsep. Same shots in the X-point scanning experiment have been added into Fig. 2, which indicated the configuration of the lower threshold power is closer to double-null configuration. Toroidal field of the discharges included in this study is anti-clockwise. Only the upper single-null configuration is with the ion grad-B drift in the favourable direction for H-mode access, that is pointing towards the X-point. Therefore threshold power with resembling double-null configuration should be lower than that with lower single-null configuration.

3 Structure of ELM

Linear BOUT++ simulation results of EAST using the data in 2010 have already been reported[24]. The simulated width is about 6cm, which has been divided into 516. The simulation resolution is 512 × 128 × 64. BOUT++ is an initial value code. The linear

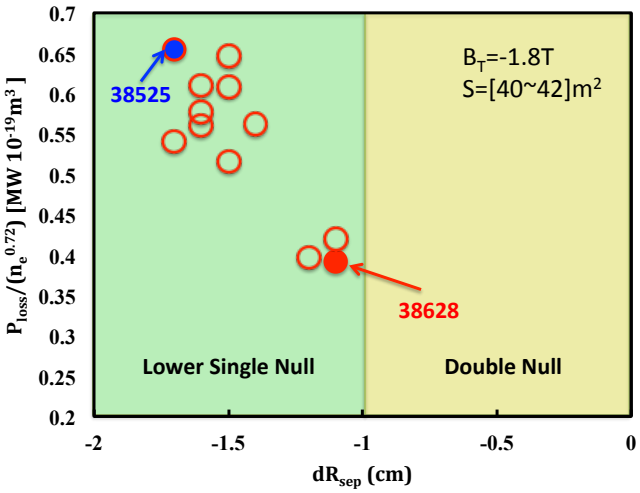

FIG. 2: Threshold power as a function of plasma density n_e with toroidal field B_T=1.6T. Red open circle is 2010 data with graphite wall, and blue solid square is 2012 data with Molybdenum wall. The solid black line is the threshold power at 1.6T predicted by the scaling law (P_{thr_cal08}).

growth is defined on

$$\gamma = \frac{d}{dt} \ln \langle P_{rms} \rangle \,, \tag{2}$$

where $\langle P_{rms} \rangle$ is the rms value of pressure perturbation.

In order to study how the plasma current affects the ELM growth rate and give more implications for the next EAST experiment, the plasma current profile has been changed while the pressure profile remains the same. Three groups of data with plasma currents of 0.5MA, 0.75MA, and 1MA have been used as the inputs for the simulation. Growth rate at low toroidal mode number (below 30) has a remarkable increase with the plasma current as shown in Fig. 3, which shows a clear signature of the current gradient driven resistive peeling modes at low-n. It also shows that the instability of the ELMs at low toroidal mode number becomes dominant when the plasma current increases.

In this campaign, plasma current has been changed from 400kA to 300kA during the H-mode phase. Figure 4 shows the filament structure of ELM from the CCD camera. From the CCD image at $I_P = 400kA$ (time=3.034s) and $I_P = 300kA$ (time=4.985s), it is obvious that the filament at $I_P = 300kA$ is much more dense than the filament at $I_P = 400kA$. Part of the image as shown in Fig. 5(a) has been selected as the input of the Fast Fourier transform. Compared with the proportion of the length of the part we selected in the length of the last closed surface, the mode number of the filament is obtained. As the safe factor $q_{95} = 4.95$, toroidal number can be calculated from the mode number as shown in Fig. 5(b). Toroidal number is 16 at $I_P = 400kA$ while is 21 at $I_P = 300kA$, which shows that higher plasma current brings the ELMs with lower toroidal number which is in agreement with the simulation.

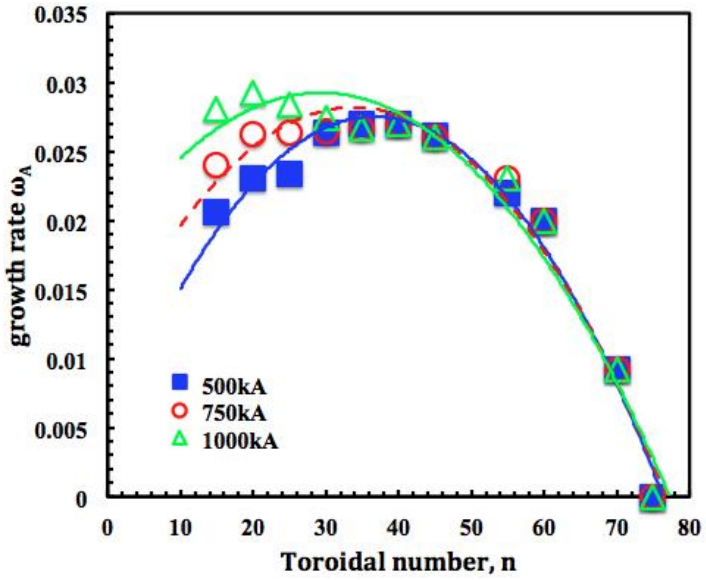

FIG. 3: Linear growth rate vs. toroidal mode number n with different plasma current and diamagnetic drift for Lunguist number $S = 10^6$.

4 Summary

Experimental threshold power in 2012 EAST campaign is lower than the scaling law, and resembling double-null configuration have advantages on achieving L-H transition. Molybdenum wall and the anti clockwise toroidal field might be the reason. Plasma current helps the generation of the ELM at low toroidal mode number which has been demonstrated both in BOUT++ simulation and CCD camera in the experiment. The toroidal number with different plasma current has been calculated. The X-point simulation and toroidal-number simulation by BOUT++ will carry though in the future.

5 Acknowledgements

This work was supported by the National Magnetic Confinement Fusion Science Program of China (No. 2010GB106000 and 2010GB106001), and the National Natural Science Foundation of China (No. 11021565).

References

[1] Wagner F. et al Phys. Rev. Lett. 53 1453 (1982)

[2] Chang C. S. et al., 2002 Phys. Plasmas, Vol. 9, No. 9

[3] Horton L. D. et al., 2000 Plasma Phys. Control. Fusion 42 A37–49

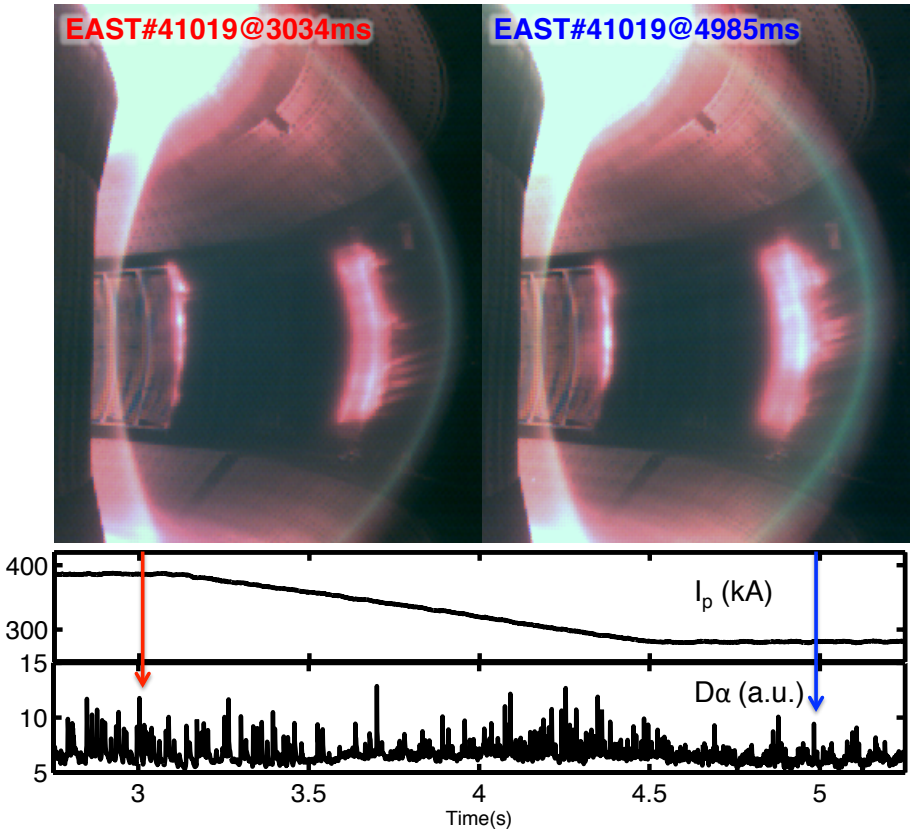

FIG. 4: CCD image at time=3.034s and 4.985s.

[4] Andrew Y. et al., 2004 Plasma Phys. Control. Fusion 46 A87

[5] Maingi R. et al., Nucl. Fusion 50 064010 (2010)

[6] Ma Y. et al., 2012 Nucl. Fusion 52 023010

[7] Z. X. Liu, X. Gao et al., Plasma Phys. Control. Fusion 54 085005 (2012)

[8] P. B. Snyder, H. R. Wilson, J. R. Ferron, L. L. Lao, A. W. Leonard, T. H. Osborne, A. D. Turnbull, D. Mossessian, M. Murakami, and X. Q. Xu, Phys. Plasmas, **9**, 2037 (2002).

[9] X. Q. Xu, B. Dudson, P. B. Snyder, M. V. Umansky, and H. Wilson, Phys. Rev. Lett., **105**, 175005 (2010).

[10] P. B. Snyder, N. Aiba, M. Beurskens, R. J. Groebner, L. D. Horton, A. E. Hubbard, J. W. Hughes, G. T. A. Huysmans, Y. Kamada, A. Kirk, C. Konz, A. W. Leonard, J. Lnnroth, C. F. Maggi, R. Maingi, T. H. Osborne, N. Oyama, A. Pankin, S. Saarelma, G. Saibene, J. L. Terry, H. Urano and H. R. Wilson, Nucl. Fusion, **49**, 085035 (2009).

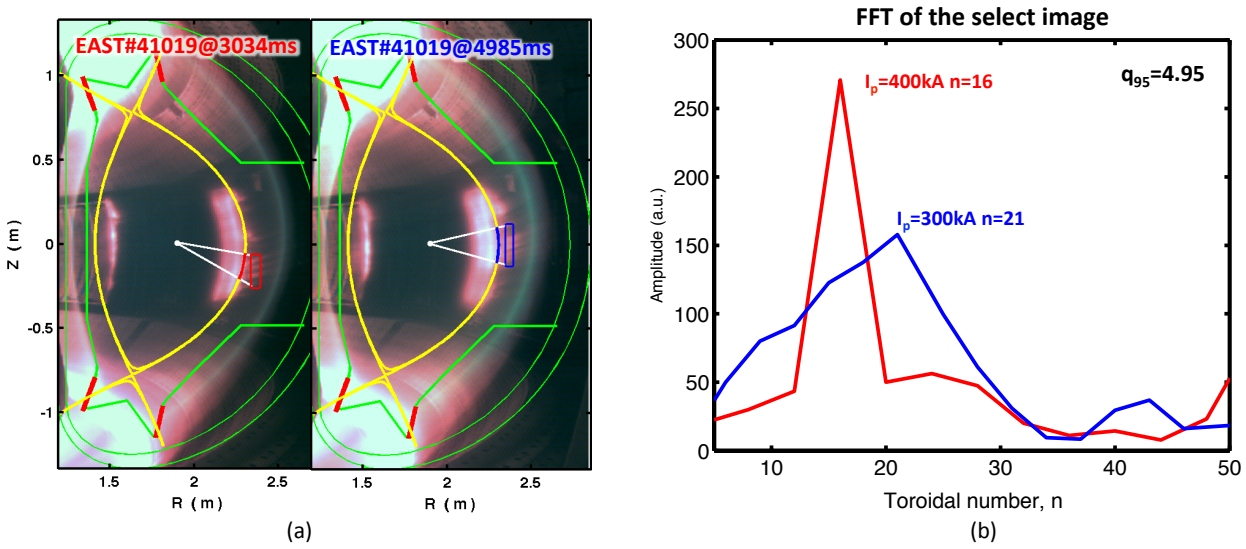

FIG. 5: Fast Fourier transform has been used to calculate the toroidal number. (a) The blue and red box is the image selected as the input of the FFT. (b) Amplitude from FFT vs. toroidal mode number n.

[11] H. R. Wilson, P. B. Snyder, G. T. A. Huysmans, and R. L. Miller, Phys. Plasmas, **9**, 1277 (2002).

[12] L. C. Bernard, F. J. Helton and R. W. Moore, Comput. Phys. Commun., **24** 377 (1981).

[13] C. R. Sovinec, A. H. Glasser, T. A. Gianakon, D. C. Barnes, R. A. Nebel, S. E. Kruger, D. D. Schnack, S. J. Plimpton, A. Tarditi, M. S. Chu, and the NIMROD Team, J. Comput. Phys., **195**, 355 (2004).

[14] D. P. Brennan, S. E. Kruger, D. D. Schnack, C. R. Sovinec and A. Pankin, J. Phys. Conf. Ser., **46**, 63 (2006).

[15] P. B. Snyder, H. R. Wilson and X. Q. Xu, Phys. Plasmas, **12**, 056115 (2005).

[16] P. B. Snyder, H. R. Wilson and X. Q. Xu, Nonlinear 3D simulations of ELMs with the BOUT code Fluid Modelling of ELMs Workshop (Boulder, CO, USA), (2006).

[17] G. T. A. Huysmans and O. Czarny, Nucl. Fusion, **47**, 659 (2007).

[18] X. J. Zhang, Y. P. Zhao, B. N. Wan, X. Z. Gong, Y. Z. Mao, S. Yuan, D. Y. Xue, L. Wang, C. M. Qin, S. Q. Ju et al 2012 Nucl. Fusion **5** 032002

[19] X. Q. Xu, B. D. Dudson, P. B. Snyder, M. V. Umansky, H. Wilson and T. Casper, Nucl. Fusion, **51**, 103040 (2011).

[20] Q. Zang, J. Y. Zhao, L. Yang, Q. S. Hu, Y. Q. Jia, T. Zhang, X. Q. Xi, S. H. Bhatti and X. Gao, Plasma Science & Technology, **12**, 144 (2010)

[21] Martin Y.R. et al J. Phys.: Conf. Ser. **123** 012033 (2008)

[22] Martin Y. R. and H-Mode Threshold Database Group 2005 Proc. of the 20th IAEA Conference Fusion Energy (CD-Rom), Vilamoura, Portugal, November vol IAEA-CSP-25/CD (Vienna: IAEA) pp IAEA–CN–116/IT/P3–35

[23] A. E. Hubbard, J. W. Hughes, I. O. Bespamyatnov, T. Biewer, I. Cziegler, B. LaBombard, Y. Lin, R. McDermott, J. E. Rice, W. L. Rowan, J. A. Snipes, J. L. Terry, S. M. Wolfe, S. Wukitch, and The Alcator C-Mod Group, Phys. Plasmas **14**, 056109 (2007)

[24] Z. X. Liu, T. Y. Xia, X. Q. Xu, X. Gao et al., "ELMy H-mode linear simulation with 3-field model on EAST tokamak using BOUT++", Phys. Plasmas (submitted), (2012)